Incorporating Protein Gradient into Electrospun Nanofibers As Scaffolds for Tissue Engineering

Jian Shi,[†,‡] Li Wang,[†,‡] Fan Zhang,[†] Hao Li,[†] Lei Lei,[†] Li Liu,[‡] and Yong Chen*[,†,‡]

Ecole Normale Supérieure, CNRS-ENS-UPMC UMR 8640, 24 rue Lhomond, 75005 Paris, France, and Institute for Integrated Cell-Material Science (iCeMS), Kyoto University, Kyoto 606-8507, Japan

ABSTRACT We report a simple but straightforward approach to produce nanofiber scaffolds with incorporated protein gradient for cell culture studies. Standard electrospinning technique was used to fabricate a high-porosity random fiber matrix. Protein molecules were then deposited in the fiber matrix by a controlled filling method, allowing the generation of a concentration gradient on the sample. When cultured with NIH 3T3 cells, it was found that the cell population on the fiber matrix depends strongly on the protein concentration. The cell morphology observation also showed the effect of the hybrid system containing both a fibrillar network and surface-coated protein gradient, revealing a different behavior of cell spreading in comparison with the experimental data of cell culture without fibers or without protein gradient.

KEYWORDS: electrospinning • nanofibers • protein gradient • tissue engineering

INTRODUCTION

Design and fabrication of functional biomaterials are important for the advanced study in tissue engineering and regenerative medicine (1−3). Ideally, the fabricated biomaterials should be able to promote cellular attachment, migration, proliferation, and controlled differentiation in vitro and to regenerate or replace damaged tissue in vivo (4, 5). Although a wide range of bulk materials including metals, inorganic compounds, polymers, and composites are now available for body implants, biomimetic scaffolds that favor nutrient diffusion, cell migration, and tissue repairing are more demanding for both fundamental research and prospective applications (6, 7). Many approaches have been proposed to generate such scaffolds, including emulsion freeze-drying, gas foaming, phase separation, leaching, etc. (8−11). Although these methods can be used to provide highly ordered three-dimensional structures, they are not sufficiently flexible to produce biomimetic structures of native extra-cellular-matrix (ECM), which possess often fibrillar architectures (12, 13). Compared to these methods, electrospinning is much more suited for the creation of scaffolds with fibrous morphology.

The electrospun fibers have large surface to volume ratio, increased porosity and good mechanical properties. They can also be re-engineered into different shapes, providing an easy access of the nanoscale analogy of the natural ECM (14, 15). Fibrous polymer matrix such as poly(lactid acid) (PLA) and poly(lactic-*co*-glycolic acid) (PLGA) produced by electrospinning have been widely used for cell culture studies (16, 17). However, such fibrous architectures alone are not sufficient for mimicking the complex natural ECM. Surfaces bearing favorable functionalities (hydrophilic, biomolecule coated, etc.) are generally needed for cell culture studies. As example, plasma treatment is frequently used for the modification of the wetting properties of the fibers scaffolds, chemical reaction or grafting is more generally used for the biomolecule attachment on the fibers surface (18, 19).

This homogeneous modification does improve the performance of the scaffold for cell adhesion and proliferation. For many other purposes, such as cell migration and network formation, the control of spatial and temporal signaling is also important. It is known that the traction force involved during cell movement is usually mediated by multiple signal cascades (20). For these reasons, development of scaffolds displaying a surface-bound gradient will be a general goal of next-generation tissue engineering. One of the approaches is to generate concentration gradients of bioactive molecules in appropriate scaffolds, which allows a heterogeneous distribution of cells or growth factors.

In this paper, we propose a facile method to generate biomolecule gradients on electrospun fibers matrix by controlled wet filling with protein solutions. The fibers matrix was first produced by electrospinning of a polymer solution on indium tin oxide (ITO) glass substrate. The sample was then put vertically in a fluidic chamber made of polydimethylsiloxane (PDMS). Protein solution was injected from bottom to fill the chamber. As the amount of protein molecules deposited is proportional to the immersion time, a protein gradient along the axis of the substrate can be generated by varying the filling speed. After optimization, NIH 3T3 cells were cultured on the protein gradient incorporated fiber scaffold. Cell responses to the gradient were

* Corresponding author. E-mail: yong.chen@ens.fr.
Received for review November 16, 2009 and accepted March 3, 2010
† Ecole Normale Supérieure.
‡ Kyoto University.
DOI: 10.1021/am9007962

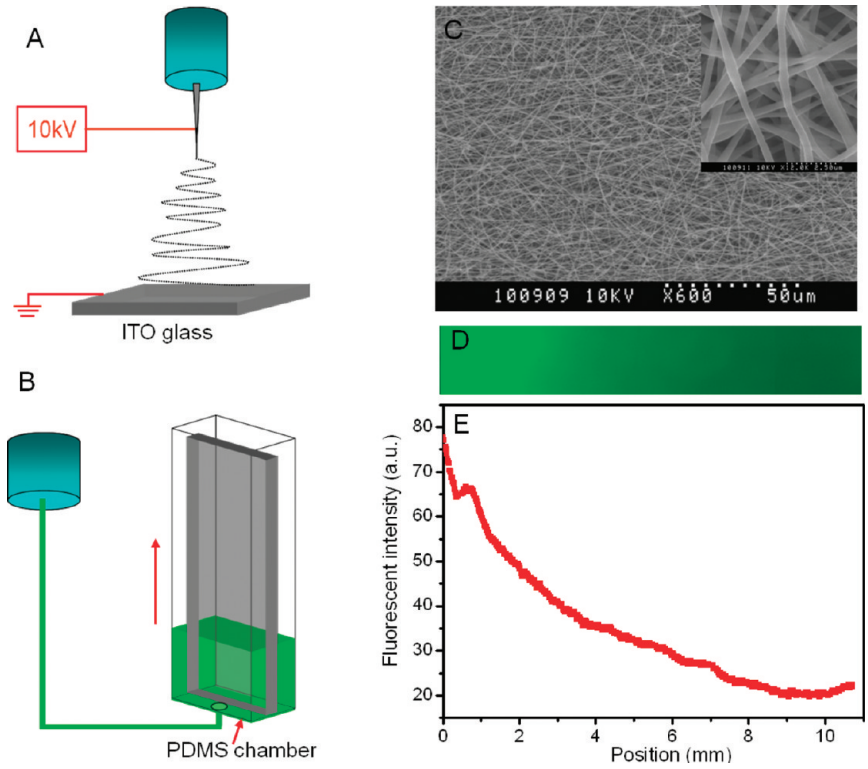

FIGURE 1. Electrospinning of nanofibers and deposition of protein gradient: (A) polymer fibers were deposited on an ITO glass slide; (B) protein gradient was generated on the fiber layer by speed controlled filling; (C) scanning electronic micrograph (SEM) of randomly deposited PMGI fibers; (D) fluorescent micrograph of the slide after filling with a solution of FITC-labeled fibronectin for a total length of about 10 mm; (E) corresponding fluorescence intensity profile of the fiber-coated slide.

then recorded and analyzed, showing application potential of the hybrid system for tissue engineering purposes.

EXPERIMENTAL SECTION

Our fabrication process consists of two steps (Figure 1A,B): (1) electrospinning of nanofibers on an ITO glass substrate and (2) generation of protein gradient on the nanofiber-coated samples. The fabricated samples are then used for cell culture and characterization.

Electrospinning. A solution of polymethylglutarimide (PMGI) at 11% in tetrahydrofuran (THF) and cyclopentanone was purchased from Microchem Corp (Germany). To obtain smooth and homogeneous fibers, was added a solution of sodium dodecyl sulfate (SDS) in ethanol in with a final concentration of 0.48 g/L. Custom electrospinning apparatus was built to obtain random PMGI nanofibers. The polymer solution was loaded with a syringe to a stainless steel needle (18 gauge). The needle was connected to a high voltage supply (Heinzinger Electronic, Germany). A small piece of ITO glass (1 cm × 0.5 cm) was used as collector. Electrospinning was performed with a voltage of 10 kV. The flow rate of the syringe pump was 8 μL/min and the distance between the needle and the collector was 10 cm. All samples were prepared with the same deposition time (1 min).

Gradient Formation. A fluidic chamber was specially designed for the protein deposition with gradient. First, two PDMS layers of 1 and 0.2 cm thickness were prepared by casting a PDMS mixture (1:10) on flat silicon wafers. After curing at 80 °C for 1 h and peeling them off, a slender cuboid chamber of 0.5 cm × 1 cm × 1 cm was made in the thick PDMS layer by cutting. A hole was pinched in the thin PDMS as entrance for solution injection. After oxygen plasma treatment, the two PDMS layers were bonded at 80 °C for 30 min. The assembly was then held upright and the fiber-coated substrate was placed into the chamber vertically. The fibronectin containing solution was then injected into the chamber through the inlet at the bottom of the system with a programmable syringe pump. The flow stopped once the chamber was fulfilled. By controlling the filling speed, the immersion time of the samples could be controlled. Finally, NIH 3T3 cells were cultured on the gradient integrated fiber matrix.

NIH 3T3 Cell Culture and Staining. NIH 3T3 cells were cultured in the 5% CO_2 incubator on a tissue culture flask. They were then dissociated with 0.25% Trypsin-EDTA solution at 37 °C for 3 min. After centrifugation, cells were resuspended in the medium at the density of 1 × 10^6/mL and 100 μL cell solution was put onto the samples. After cell loading and culturing for 24 h, cells were fixed with 4% formaldehyde PBS solution for 20 min, permeabilized in 0.5% Triton-X-100 PBS solution for 10 min, blocked with a PBS solution with 3% BSA and 0.1% Triton-X-100 for 1 h, incubated with Phalloidin-FITC (1 μg/mL) and DAPI (100 ng/mL) for 20 min, and finally washed three times with PBS.

Characterization. Cell cytoskeleton investigated with the fluorescence images were taken with a fluorescence microscope (Zeiss Axiovert 200) equipped with a CCD camera (Q-imaging, Burnaby, British Columbia, Canada). The high-resolution observation was performed with a scanning electron microscope (Hitachi S-800) operated at 8 kV. For cell morphology observation, samples were first fixed in a solution containing 2.5% glutaraldehyde and 4% phosphate-buffered saline (PBS) for fixation for 30 min. The samples were then rinsed twice with PBS buffer and immersed in 70% ethanol (in DI) for 30 min. Afterward, the samples were dehydrated in a graded series of ethanol with concentrations of 30, 50, 70, 80, 90, 95, and 100%, respectively, each for 10 min and dried with a nitrogen gas flow. Before observation, a 5 nm thick gold layer was deposited on the samples by sputtering.

RESULTS AND DISCUSSIONS

Preparation of PMGI Fibers. PMGI polymer has been chosen for the fabrication of nanofibers because of its good biocompatibility, high surface energy, and stiffness (21). Our previous attempts showed, however, quite nonuniform fibers deposition and the formation of a large amount of beads inside the fiber matrix (22). To avoid this effect, we added in this work surfactant SDS in the PMGI solution in hoping that the presence of the surfactant can increase the surface charge density so that the bead formation can be reduced by charge repulsion. Figure 1C shows a typical fiber matrix deposited on an ITO glass slide by electrospinning. As can be seen, the fabricated fibers are homogeneous and bead free, with an average diameter about 300 nm.

The fibers deposited by electrospinning are generally not well fixed on the substrate and they detached easily when immersed in liquid. In practice, experiences with cell culture, fixation, staining and characterization involve multistep exchanges with different solution and water rinsing so that it is important to find a solution to improve the fibers attachment on the substrate. One solution is to heat slightly above the glass transition temperature of the polymer fibers. For PMGI fibers, such a thermal treatment was performed on a 190 °C hot plate for 1 min. Because the surface of the deposited PMGI polymer scaffolds is also hydrophobic, it could not be used directly for cell culture. After thermal fixation and before cell seeding, the sample was immersed in pure ethanol solvent for 30 min, giving an improved wetting ability due to the introduction of −OH group.

Preparation of Fibronectin Gradient. The electrospun fibrous scaffolds provide topographical cues for cell culture. Additional treatment by surface coating of the fibers with appropriate bio molecules (gelatin, collagen, etc.) can further improve the cell-material interaction (23, 24). Recently, Li et al. demonstrated fibers scaffold with a surface stiffness gradient of calcium phosphate, allowing mimicking the tendon-to-bone insertion site (25). This kind of hybrid scaffold may also be useful for the cell polarity and cell migration studies, which were mostly based on the physical or chemical patterns generated on a flat surface. In the case of fiber-coated substrates, it is more difficult to apply conventional lithography techniques because of the porous structures of the fibers. Therefore, we proposed a simple liquid filling method with a fluidic chamber. This method is flexible and versatile because it can work for any type of substrate and dimensions. For demonstration, FITC-labeled fibronectin solution (0.05 mg/mL) was used to generate concentration gradient on electrospun fibers with a liquid filling speed at 0.1 mm/min. Figure 1D,E showed fluorescent image of fibronectin gradient with a total immersion length of about 10 mm (D) and the corresponding fluorescent density profile along the gradient direction (E), respectively.

The amount of the fibronectin proteins deposited in the fiber scaffold is a function of the immersion time and the protein concentration of the solution. In our approach, we changed both liquid filling speed and concentration of the fibronectin. With the given volume of the PDMS chamber,

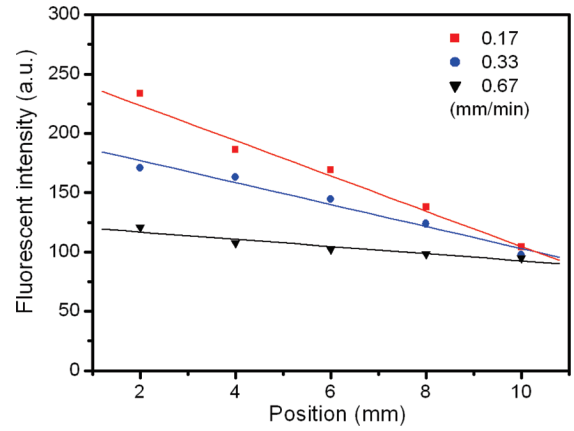

FIGURE 2. Variation in the fluorescence intensity of fiber-coated slides after filling with a 1 mg/mL fibronectin solution for three different moving speeds of the solution level.

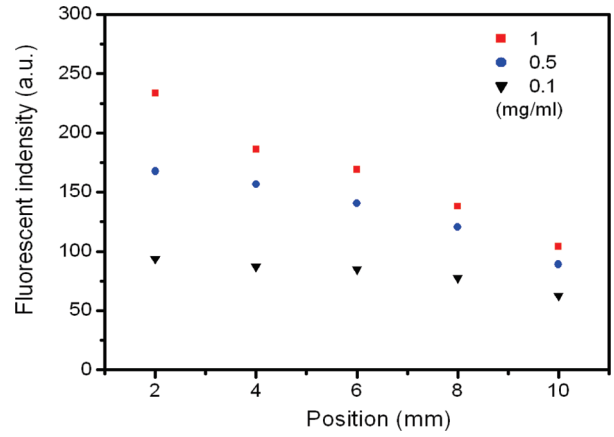

FIGURE 3. Variation in the fluorescence intensity of fiber-coated slides after filling with fibronectin solution of three different concentrations but the same moving speed of the solution level (0.17 mm/min).

1 mg/mL fibronectin solution was filled in the chamber for 15, 30, and 60 min, respectively, which corresponds to a liquid moving speed at 0.67, 0.33, and 0.17 mm/min. Figure 2 shows the fluorescence intensity versus the slide position of gradient prepared at the three filling conditions. In all cases, a roughly linear decrease in fluorescent intensity profile was observed. However, when the liquid level raised too fast (0.67 mm/min), the resulted gradient and the amount of deposited proteins were too small for meaningful observation. We also used fibronectin solution of three different concentrations (0.1, 0.5, and 1 mg/mL) to prepare a gradient with the same liquid moving speed (0.17 mm/min). The fluorescence intensity profile was plotted in Figure 3. Clearly, a low concentration resulted in a weak adsorption as well as a slow variation of the protein concentration. To obtain a better gradient profile with low concentrations, the liquid filling speed should also be sufficiently low (see Figure 1E).

Cell Response. After generation of the protein gradient on the electrospun fibers with a 1 mg/mL fibronectin solution and a liquid level moving speed of 0.17 mm/min, the sample was used as scaffolds for culturing NIH 3T3 cells, which are often used for investigation of cell adhesion and migration. To compare the cell adhesion behaviors, control experiment

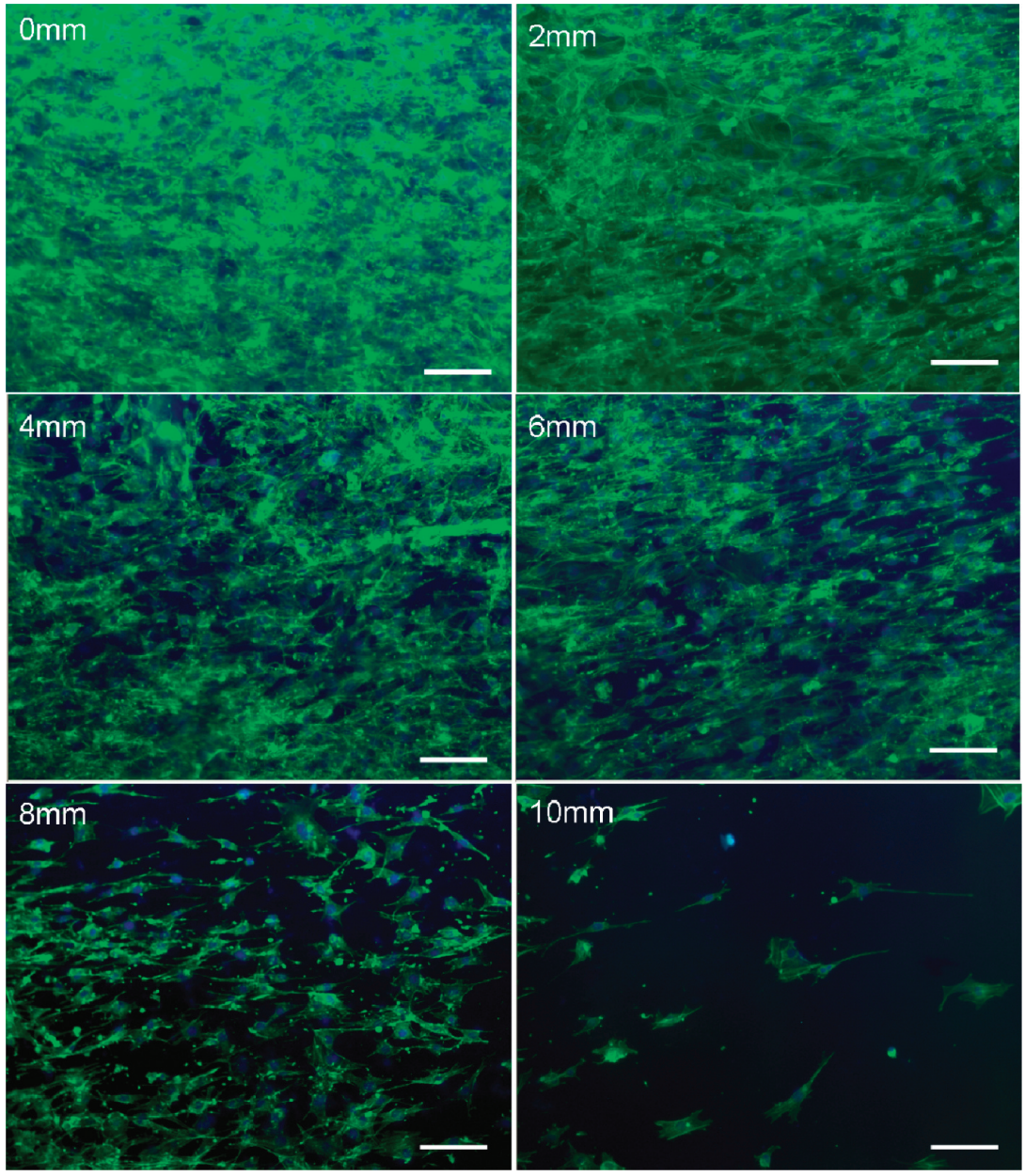

FIGURE 4. Fluorescent images of NIH 3T3 cells cultured on the surface of fiber-coated slides after 24 h. The images were taken from different regions along the fibronectin gradient (from bottom to up). Scale bar: 100 μm.

was performed under the same condition on the electrospun fibers without chemical treatment. After 24 h, cells were fixed and stained with DAPI (blue) and Phalloidin-FITC (Green), respectively, for fluorescent microscopic imaging of cell nuclei and F-actin. The result shows that on the electrospun fibers without chemical treatment, almost no cells attached on the fibers matrix (data not shown). On the sample with protein gradients, cells adhered and spread well on the fibers. Figure 4 shows a set of fluorescent images taken at different position along the gradient direction. We noted that the cell density at different region presented clear distinction. The higher fibronectin concentration located region, the higher of cell density exhibited. In the low-concentration region, only a few cells were observed. The variation of the average cell density along the gradient axis was plotted in Figure 5. This profile shows a quasilinear

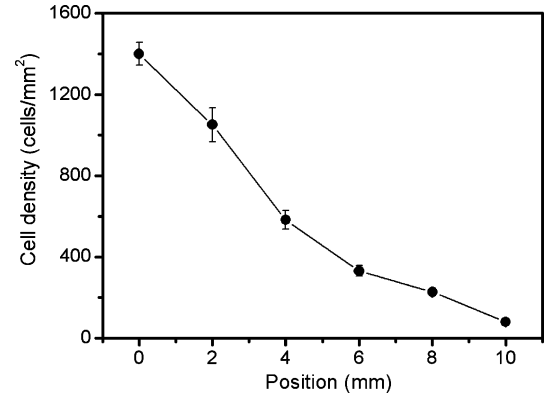

FIGURE 5. Averaged density of NIH 3T3 cells cultured on the surface of a fiber-coated slide after filling with a 1 mg/mL fibronectin solution with a solution level moving speed of 0.17 mm/min.

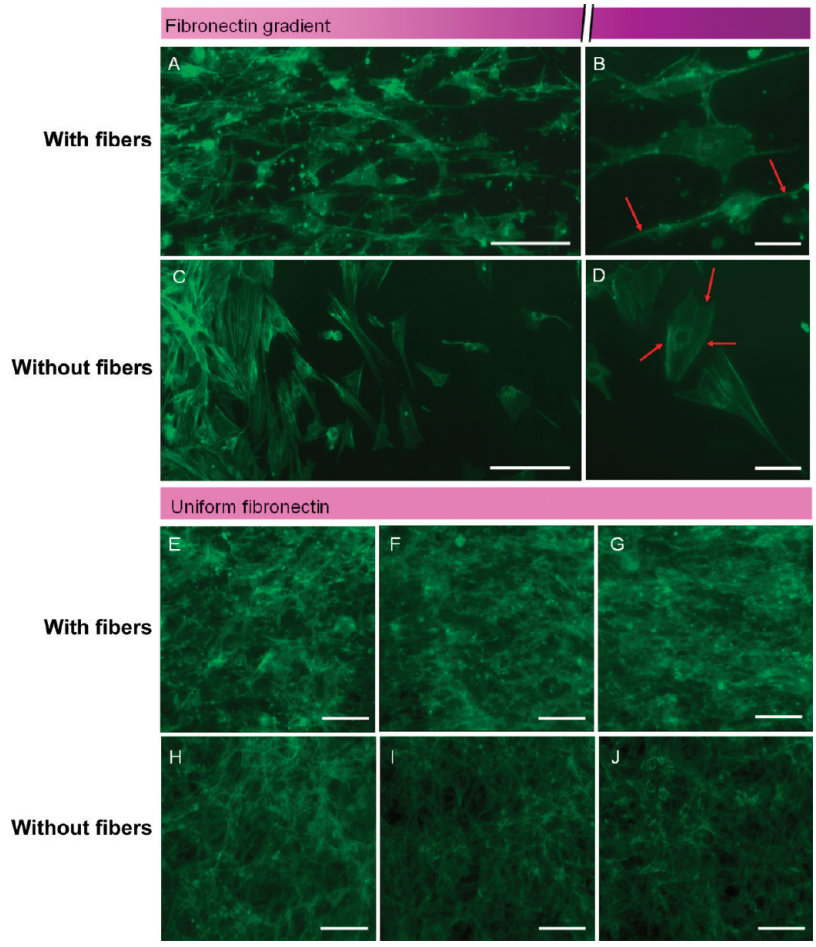

FIGURE 6. Morphology of NIH 3T3 cells on different types of surfaces: (A, B) low-concentration region on the nanofibers scaffold; (C, D) low-concentration region on the ITO glass without fiber matrix; (E, G) three different regions on the fiber matrix with uniform protein concentration; (H, J) three different regions on the flat ITO glass with uniform protein concentration. Cells were stained with Phalloidin-FITC (green) to show F-actin. The red arrow indicates the distribution of F-actin distribution. The two pink rectangle bars on top and in the middle of the images indicates the surface concentration of fibronectin. Scale bar: (A, C) 100, (B, D) 20, and (E–J) 100 μm, respectively.

dependence of the NIH3T3 cell density on the fibronectin concentration. The cell morphologies on the fibers were characterized by scanning electronic microscope observation (see the Supporting Information, Figure S1). In the high-concentration region, a large number of cells could be found that were connected to each other and spread over large areas on top of the fiber matrix. In the low-concentration region, fewer cells could be observed, showing small tails clearly stretched out from the cell body and bounded on the fiber interface. These differences in cell morphology revealed that on the one hand, a high density of fibronectin molecules leads to a better cell attachment with an increased cell density. On the other hand, the fiber matrix plays more important role to guide the formation of cellular patterns. Thus, both the chemical and physical cues played important roles for cell activities.

The actin filaments of NIH 3T3 cells at the obvious transient position could also be observed. Figure 6A, B show the fluorescence images of cells on the gradient decorated fibers (8 mm from bottom). Clearly, cells exhibited an elongated tendency toward the high concentration region. They formed long and sharp tails in front and end of the cell bodies. Uniform actin fibers were found along the cell axis. The control experiment has been done on an ITO glass substrate with protein gradient but without fibers, showing broadened lamellipodia and actin fibers around the cell periphery as shown in Figure 6C, D. Accordingly, the elongation degree of the cell bodies decreased significantly. To demonstrate the effect of the protein gradient, we imagined NIH 3T3 cells on the ITO glass substrate with (Figure 6E, G) or without fibers (Figure 6H–J) but both uniformly coated with fibronectin (1 mg/mL). As expected, homogeneous cell distribution could be observed in both cases, proving that the protein gradient is responsible to the cell morphology changes. The protein gradient can also be responsible to the cell polarity and the cell migration. Indeed, in our experiments, cells clearly elongated toward the high-concentration region on the hybrid scaffolds. Time lapse experiments are needed for the investigation of cell migration behaviors.

CONCLUSION

We have developed a simple method for the generation of protein gradient on electrospun nanofibers. The whole fabrication process is flexible and versatile without using any expensive or sophisticated equipment. By controlling the immersion time and the fibronectin concentration, we could generate the desired biochemical gradient for suitable cell culture and migration studies. The performance of the

fabricated scaffold was demonstrated by culturing NIH3T3 cells. We have shown that the electrospun nanofibers matrix facilitate tissue formation. We also demonstrated that the presence of the protein gradient can not only improve the cell-scaffold interaction but also affect the cell spreading behaviors. Thus, the proposed hybrid scaffolds could be used for advanced tissue engineering studies.

Acknowledgment. This work was supported by European Commission through project contract CP-FP 214566-2 (Nanoscales), and the French National Research Agency through project contract ANR-06-NANO-028-03 (Active Nanopore). J.S. is grateful to the region of Ile-de-France for a grant (Program DIM Cells and Stem Cells). The content of this work is the sole responsibility of the authors.

Supporting Information Available: Figures showing cell morphology observed by scanning electronic microscopy (SEM) (PDF). This material is available free of charge via the Internet at http://pubs.acs.org.

REFERENCES AND NOTES

(1) Langer, R.; Vacanti, J. P. *Science* **1993**, *260*, 920–926.
(2) Khetani, S. R.; Bhatia, S. N. *Curr. Opin. Biotechnol.* **2005**, *17*, 524–531.
(3) Stupp, S. I. *MRS Bull.* **2005**, *30*, 546–553.
(4) Ma, P. X. *Mater. Today* **2004**, *7*, 30–40.
(5) Freed, L. E.; Engelmayr, G. C.; Borenstein, J. T.; Moutos, F. T.; Guilak, F. *Adv. Mater.* **2009**, *21*, 1–9.
(6) Tsang, V. L.; Bhatia, S. N. *Adv. Drug. Deliv. Rev.* **2004**, *56*, 1635–1647.
(7) Moroni, L.; Elisseeff, J. H. *Mater. Today* **2008**, *11*, 44–51.
(8) Whang, K.; Goldstick, T. K.; Healy, K. E. *Biomaterials* **2000**, *21*, 2545–2551.
(9) Yoon, J. J.; Park, T. G. *J. Biomed. Mater. Res.* **2001**, *55*, 401–408.
(10) Liu, X. H.; Ma, P. X. *Biomaterials* **2009**, *30*, 4094–4103.
(11) Levenberg, S.; Huang, N. F.; Lavik, E.; Rogers, A. B.; Itskovitz-Eldor, J.; Langer, R. *Proc. Natl. Acad. Sci. U.S.A.* **2003**, *99*, 12741–12746.
(12) Barnes, C.; Sell, S.; Boland, E.; Simpson, D.; Bowling, G. *Adv. Drug Delivery Rev.* **2007**, *59*, 1413–1433.
(13) Janmey, P.; Winer, J. P.; Weisel, J. W. *J. R. Soc. Interface* **2009**, *6*, 1–10.
(14) Nisbet, D. R.; Forsythe, J. S.; Shen, W.; Finkelstein, D. I.; Horne, M. K. *J. Biomater. Appl.* **2009**, *24*, 7–29.
(15) Teo, W. E.; He, W.; Ramakrishna, S. *Biotechnol. J.* **2006**, *1*, 918–929.
(16) Badami, A. S.; Kreke, M. R.; Thompson, M. S.; Riffle, J. S.; Goldstein, A. S. *Biomaterials* **2006**, *27*, 596–606.
(17) Xin, X.; Hussain, M.; Mao, J. J. *Biomaterials* **2007**, *28*, 316–325.
(18) Shabani, I.; Haddadi-Asl, V.; Seyedjafari, E.; Babaeijandaghi, F.; Soleimani, M. *Biochem. Biophys. Res. Commun.* **2009**, *382*, 129–133.
(19) Edlund, U. E.; Källrot, M.; Albertsson, A. *J. Am. Chem. Soc.* **2005**, *127*, 8865–8871.
(20) Phillips, J. E.; Burns, K. L.; Le Doux, J. M.; Guldberg, R. E.; Garcia, A. J. *Proc. Natl. Acad. Sci. U.S.A.* **2008**, *105*, 12170–12175.
(21) Liu, L.; Shi, J.; Yuan, Q. H.; Wang, L.; Jung, D.; Nakatsuji, N.; Chen, Y., submitted.
(22) Shi, J.; Wang, L.; Chen, Y. *Langmuir* **2009**, *25*, 6015–6018.
(23) Ma, Z.; He, W.; Yong, T.; Ramakrishna, S. *Tissue. Eng.* **2005**, *11*, 1149–1158.
(24) Li, W. S.; Guo, Y.; Wang, H.; Shi, D. J.; Liang, C. F.; Ye, Z. P.; Qing, F.; Gong, J. *J. Mater. Sci. Mater. Med.* **2008**, *19*, 847–854.
(25) Li, X. R.; Xie, J. W.; Lipner, J.; Yuan, X. Y.; Thomopoulos, S.; Xia, Y. N. *Nano Lett.* **2009**, *9*, 2763–2768.

AM9007962